PENNSTATE

Applied Research Laboratory

# A FLUORESCENCE TECHNIQUE FOR MEASUREMENT OF SLOT INJECTED FLUID CONCENTRATION PROFILES IN A TURBULENT BOUNDARY LAYER

**T.A. Brungart**
**H.L. Petrie**

Technical Memorandum
File No. 90-197
27 August 1990

Copy No. 6



Approved for Public Release. Distribution Unlimited.

Applied Research Laboratory
P.O. Box 30
State College, PA 16804
(814) 865-3031

# REPORT DOCUMENTATION PAGE

| | |
|---|---|
| 1a REPORT SECURITY CLASSIFICATION<br>Unclassified | 1b. RESTRICTIVE MARKINGS |
| 2a. SECURITY CLASSIFICATION AUTHORITY | 3 DISTRIBUTION / AVAILABILITY OF REPORT |
| 2b DECLASSIFICATION / DOWNGRADING SCHEDULE | |
| 4 PERFORMING ORGANIZATION REPORT NUMBER(S)<br>TM 90-197 | 5. MONITORING ORGANIZATION REPORT NUMBER(S) |
| 6a NAME OF PERFORMING ORGANIZATION<br>Applied Research Laboratory<br>6b OFFICE SYMBOL *(If applicable)* | 7a. NAME OF MONITORING ORGANIZATION |
| 6c ADDRESS *(City, State, and ZIP Code)*<br>Post Office Box 30<br>State College, PA 16804 | 7b. ADDRESS *(City, State, and ZIP Code)* |
| 8a NAME OF FUNDING / SPONSORING ORGANIZATION<br>David Taylor Research Center<br>8b OFFICE SYMBOL *(If applicable)* | 9. PROCUREMENT INSTRUMENT IDENTIFICATION NUMBER |
| 8c ADDRESS *(City, State, and ZIP Code)*<br>Department of the Navy<br>Bethesda, MD 20084 | 10 SOURCE OF FUNDING NUMBERS<br>PROGRAM ELEMENT NO. / PROJECT NO / TASK NO. / WORK UNIT ACCESSION NO. |

11 TITLE *(Include Security Classification)*
A Fluorescence Technique for Measurement of Slot Injected Fluid Concentration Profiles in a Turbulent Boundary Layer

12 PERSONAL AUTHOR(S)
T. A. Brungart and H. L. Petrie

| 13a TYPE OF REPORT | 13b TIME COVERED FROM _____ TO _____ | 14. DATE OF REPORT *(Year, Month, Day)* | 15. PAGE COUNT |
|---|---|---|---|
| | | | 33 |

16 SUPPLEMENTARY NOTATION

| 17 COSATI CODES | | | 18 SUBJECT TERMS *(Continue on reverse if necessary and identify by block number)* |
|---|---|---|---|
| FIELD | GROUP | SUB-GROUP | |
| | | | |
| | | | |

19 ABSTRACT *(Continue on reverse if necessary and identify by block number)*

A technique for measuring near instantaneous concentration profiles of a fluid injected through a narrow inclined slot at the wall into a high unit Reynolds number flat plate turbulent boundary layer is discussed. The concentration profiles are determined by measuring the light intensity emitted from a fluorescent dye, premixed into the injectant flow, as the injectant convects through an excitation laser beam. The fluorescence intensity is quantified by an electronically shuttered single stage microchannel plate image intensifier coupled to a linear photodiode array. This instrumentation provided the high spatial and temporal resolution required for these boundary layer concentration profile measurements. The laser induced fluorescence technique is being used to study the diffusion of injected polymer solutions away from the near wall region of the boundary layer where these solutions are effective in reducing drag. The diffusion of slot injected water has also been examined and the present results are in excellent agreement with previous studies.

| | |
|---|---|
| 20 DISTRIBUTION / AVAILABILITY OF ABSTRACT<br>☐ UNCLASSIFIED/UNLIMITED ☐ SAME AS RPT. ☐ DTIC USERS | 21. ABSTRACT SECURITY CLASSIFICATION |
| 22a NAME OF RESPONSIBLE INDIVIDUAL | 22b. TELEPHONE *(Include Area Code)* / 22c. OFFICE SYMBOL |

# A FLUORESCENCE TECHNIQUE FOR MEASUREMENT OF SLOT INJECTED FLUID CONCENTRATION PROFILES IN A TURBULENT BOUNDARY LAYER

T. A. Brungart and H. L. Petrie

Technical Memorandum
File No. 90-197
27 August 1990



Originally Issued as an IM on 5 July 1990.

From: T. A. Brungart and H. L. Petrie

Subject: *A Fluorescence Technique for Measurement of Slot Injected Fluid Concentration Profiles in a Turbulent Boundary Layer*

References: See Page 21.

Abstract: A technique for measuring near instantaneous concentration profiles of a fluid injected through a narrow inclined slot at the wall into a high unit Reynolds number flat plate turbulent boundary layer is discussed. The concentration profiles are determined by measuring the light intensity emitted from a fluorescent dye, premixed into the injectant flow, as the injectant convects through an excitation laser beam. The fluorescence intensity is quantified by an electronically shuttered single stage microchannel plate image intensifier coupled to a linear photodiode array. This instrumentation provided the high spatial and temporal resolution required for these boundary layer concentration profile measurements. The laser induced fluorescence technique is being used to study the diffusion of injected polymer solutions away from the near wall region of the boundary layer where these solutions are effective in reducing drag. The diffusion of slot injected water has also been examined and the present results are in excellent agreement with previous studies.

Acknowledgements: The authors wish to acknowledge the assistance of Mr. W. L. Harbison, Dr. C. L. Merkle, and Mr. S. T. Sommer throughout the course of this work. Discussions with Prof. W. G. Tiederman and Mr. D. T. Walker at Purdue University were appreciated. This investigation was supported by the David Taylor Research Center, Mr. W. G. Souders, technical monitor.

Table of Contents

List of Figures

## INTRODUCTION

The addition of solutions of long chain polymer to wall bounded turbulent shear layers is one of the most effective drag reduction techniques known. It is generally accepted that drag reduction is a result of a suppression of eddies at the dissipation scales in the boundary layer buffer region (Lumley, 1973 and 1976). Drag reduction in external flows is achieved by injection of polymer into the near wall region, typically, through an inclined narrow slot. The turbulent diffusion of the injected polymer away from the wall as it convects downstream diminishes both the concentration near the wall and the local drag reduction levels with increasing streamwise distance. Acquiring a detailed knowledge of the polymer diffusion process, the factors influencing diffusion and the relationship between the effects of diffusion and the resulting drag reduction levels are the primary concerns of the present work. These factors were the motivation for the development of the experimental techniques discussed below.

Since the pioneering work of Toms (1949), hundreds of experiments have been conducted to study the effects of polymer additives on turbulent shear flows. A number of investigators have studied the diffusion of wall injected polymer in external boundary layer flows. Wetzel and Ripken (1970) measured mean concentration profiles of a polymer solution injected at the wall in an open channel facility. Their approach was to draw off samples through small total head probes at various locations in the turbulent boundary layer (TBL). Latto and El Riedy (1976), Collins and Gorton (1976), and Vdovin and Smol'yakov (1978, 1981), used similar probe techniques to study polymer diffusion in a flat plate TBL. Gebel et al. (1978), describes similar pipeflow

experiments. In a following study, Bues et al. (1985) used fluorescent dye to visualize wall injected polymer diffusion in a turbulent pipeflow. Fruman and Tulin (1976) studied how diffusion reduces the polymer concentration at the wall in a flat plate TBL by drawing off samples through narrow slits in the surface.

The conventional probe sampling techniques mentioned above are limited to determining the mean concentration at the probe. Additionally, these probe techniques are limited in resolution and in the approach to the wall due to the size of the sampling probe relative to the diffusion layer scales within the TBL. Also, Latto et al. (1981), has shown that these probe techniques tend to give mean values that are low and that depend on the sampling rate.

Tiederman et al. (1987), made nonintrusive mean concentration measurements in a low speed rectangular channel with slot injection of polymer. The mean concentration at a given height above the wall was determined by the attenuation of a laser beam due to absorption from a fluorescent dye premixed into the polymer. The beam was directed spanwise across the flow and parallel to the surface. Interestingly, the spanwise average was not steady and had to be temporally averaged. Spatial resolution in the direction normal to the wall is limited to the maximum laser beam diameter across the span of the polymer laden flow which was 500 microns in this case. In the present work, the viscous scales at the wall are 5 to 25 times smaller than in this channel flow and a higher resolution technique is required.

Koochesfahani and Dimotakis (1985) studied free shear layer mixing by a laser induced fluorescence (LIF) technique. The approach taken was

to direct a focused laser beam across the mixing layer normal to the approach flow with one of the flows seeded with a fluorescent dye. The local dye concentration of the fluid convecting through the excitation laser beam was determined by measuring the local fluorescence intensity.

The approach taken by Koochesfahani and Dimotakis (1985) has been adopted for the current polymer diffusion experiments with appropriate modifications for the higher velocities and smaller spatial scales of the TBL flows of interest. Both the dye and the polymer have high Schmidt numbers and as a result convect and mix as one at the scales resolved. The present techniques allow polymer concentration profile statistics to be determined and provides a dynamic visualization that has not been possible in previous TBL polymer diffusion investigations. Walker and Tiederman (1988, 1990) have taken a similar approach in their low speed channel flow studies.

## EXPERIMENTAL APPARATUS

A 1.91cm thick flat plate was mounted at the centerplane of the 0.305m diameter test section of a closed loop water tunnel at the Penn State University Applied Research Laboratory. The leading edge of the 1.2m long plate was positioned 0.1m upstream of the test section in the 9-to-1 contraction ratio inlet. Both pressure surveys and laser velocimeter surveys have been performed to establish that the boundary layer on this plate is in equilibrium and has a zero pressure gradient in the tunnel test section. Flat acrylic windows, blended smoothly into the circular test section walls, provided optical access from both sides and below the plate. The plate itself is fitted with an acrylic window to provide optical access through the plate from 0.005m to 0.46m downstream of a slot injector. Figure 1 is a scale drawing of the plate

mounted into the water tunnel. The entire test area was enclosed inside of an opaque black tent to prevent ambient light from contaminating the results.

The slot injector, of 0.191m span, is fed by a line from each side of the tunnel. The two convergent walls forming the slot are at angles of 20 and 30 degrees with the horizontal surface of the plate. The width of the slot, measured parallel to the plate at the exit of the slot, is 1.0mm. The slot is located 292mm downstream from the plate leading edge, and its distance from the boundary layer virtual origin was determined by LDV surveys to be 353mm. The small plenum in the plate below the slot assembly was loosely packed with a course non-metallic steel wool type material to provide a uniform exit flow of polymer.

The polymer was pumped from a storage container to the plenum with a small peristaltic pump. An air bubble in the supply line plumbing, with an approximate volume of 2 to 3 liters, effectively removed pump pulsations from the flow. This was verified by visual inspection and from surface flush hot-film anemometer results taken 12.7mm downstream of the injection slot.

A diagram of the LIF excitation optics used to make the polymer concentration profile measurements is presented in Figure 2. An argon ion laser provided an excitation beam at a 488nm wavelength. The laser beam was directed through the plate from the bottom window in the tunnel. With the beam directed in this manner, it is possible to properly account for excitation beam absorption along its path over the field of view of the LIF imaging optics. Also, mounting the excitation laser and optics onto a breadboard and supporting frame below the tunnel

was the most convenient and practical configuration. In all cases, beam absorption along its path from the tunnel sidewall to the plate due to the build up of a background dye concentration in the tunnel was negligible.

The fluorescence intensity change with increasing laser power for a constant uniform dye concentration was found to be linear up to 400mW, as expected, and 350mW of excitation laser power was used. The excitation laser was operated in a constant power mode that limits output power variations to less than 0.5%. The bulk of the experiments were performed with a 900mm focal length lens and a 5X beam expansion ratio to form the excitation beam. This produced a beam diameter to the $e^{-2}$ intensity level of approximately 90 microns.

The dye used, fluorescein disodium salt, has a number of advantages over other commonly used fluorescent dyes such as rhodamines. Fluorescein is highly soluble in water and has a high quantum yield, typically 85%. The dye has a weak temperature dependence relative to that of rhodamine B which can be 5% per K, Guilbault (1973). Also, rhodamines are known carcinogens. Fluorescein has a strong pH dependence in the range from 4 to 7.5, Walker (1987). In the present study, the pH of the tunnel water was 7.4 or higher and polymer solution pH ranged as high as 8.2 This range of pH changes the fluorescence signal strength by only 5%. The absorption peak of aqueous fluorescein solutions is near 490nm which is conveniently close to the 488nm wavelength available with argon ion lasers. For this reason, the 488nm wavelength was used for excitation rather than 514.5nm as was used by Koochesfahani and Dimotakis (1985). The emission spectrum peak is near 520nm.

The fluorescence intensity of solutions of water and fluorescein was observed to diminish with time. Fluorescein does not fluoresce in an oxidized state and is an effective indicator of oxidation reduction reactions, Guilbault (1973). It appears that the dye may be reacting with dissolved substances in the water. The fluorescence signal decay of polymer solutions made with polyethylene oxide or Separan AP-30 was not as rapid. Initially, dye was added to the injectant immediately prior to use to avoid these signal decay effects. However, since the fluorescence signal decay rate was observed to diminish appreciably with time, the use of aged solutions was adopted. This produced better repetition of the calibrations than the former procedure.

Fluorescent dyes continuously exposed to excitation radiation undergo a photobleaching reaction to a non-fluorescing state. The fraction of photobleached molecules per photon absorbed is the bleaching quantum efficiency, $Q_b$, and is small. Ippen, et al. (1970), has determined the bleaching efficiency to be $Q_b = 4 \times 10^{-6}$ for fluorescein exposed to light at 514.5nm wavelength. As discussed by Koochesfahani (1984), the number of dye molecules available to fluoresce decreases exponentially with a time constant given by:

$$T_b = 1/(Q_b \Phi \sigma)$$

where $\Phi$ is the photon flux in photons/cm$^2$/s, and $\sigma$ is the molecular cross section of the dye in cm$^2$. The molecular cross section is determined from the extinction coefficient, $\epsilon$, using $\sigma = 2300\ \epsilon/N_{av}$, where $N_{av}$ is Avogadro's number, Parker (1968). Using $\epsilon = 8.72 \times 10^4$/(cm(mole/liter)) for the extinction coefficient, Walker (1987), the time constant is 0.06 seconds for the present system. The transit time

of a fluid element across the laser beam is well less than this at any resolvable distance above the wall in the present TBL flows.

The LIF imaging optics for the concentration profile measurements are shown in Figure 3. The image of the fluorescing dye in the laser beam is focused onto the input window of a single stage microchannel plate image intensifier by a long range microscope. A Schott glass long pass filter with a 50% cut-off at 515nm was positioned between the microscope and the input window to eliminate scattered excitation radiation from the signal. The output phosphor screen of the image intensifier was fiber optically coupled to the input window of a 512 pixel element linear photodiode array. The array pixel dimensions are 25 microns along the axis of the excitation laser beam and 2.5mm perpendicular to the beam axis. The wide 2.5mm dimension of the array pixels allows the entire diameter of the laser beam to be imaged onto the array, even with 5X magnification and in the presence of vibration. This avoids possible non-concentration signal variation caused by partial movement of the beam image off the array.

The long range microscope in Figure 3 was used with the focal distance set at 0.75m, approximately. The microscope was a Questar QM1 and the manufacturer specifies a 3 micron resolution capability. Magnifications have been varied from 2.1 to 5.0 power in the present work at this distance. At 5 power magnification, one pixel element images a 5 micron slice of the laser beam in the flow. This equals one viscous wall unit in the TBL at a 4.6m/s test velocity, approximately. The resolution of the system is limited, however, by the image intensifier which has a full width at half modulation of 3 to 3.5 pixels based on the manufacturer's specifications and our own experimental

verification. This is partially attributed to the spreading of the electron cloud between the microchannel plate and the output phosphor screen, see Wick (1967). Based on manufacturer's specifications, blooming in the photodiode array is a relatively small part of this signal spread.

The image intensifier has a linear response for the conditions of interest, provides a luminous gain of at least 10,000, and can be electronically gated. The combination of the last two factors makes it possible to measure concentration profiles using extremely short photon integration periods. The image intensifier could be gated open to collect photons for periods from 80ns to 7ms by a high voltage pulse generator. A gate period of approximately 7.2 microseconds was used in the present study to limit the convection of fluid through the excitation beam during this photon integration period. The control unit shown in Figure 3 scanned and reset the array after each intensifier gate period. The array was scanned serially across all 512 pixels after the gated integration period and 50 to 60 array scans were sampled per second. Typically, 1000 scans were taken at each test condition which required approximately 1Mb of storage on the PC/AT computer used. A near real time display on the computer facilitated experiment set-up and monitoring.

The output window of the image intensifier is a P20 phosphor screen. An image lag between successive scans of the array may exist because the length of time for the output from the phosphor screen to decay to a negligible level may exceed the period between the scans. This was investigated by placing a mechanical shutter in the excitation laser beam while imaging the light emitted from a uniform dye solution

circulated through the calibration flow cell onto the input window of the image intensifier. The mechanical shutter allowed the excitation beam into the flow cell for a period sufficient for one gating of the image intensifier only. Subsequent scans had no input signal and would show the extent of the image lag. It was observed that the image decay between scan periods exceeded 90% for the conditions of the experiment. Therefore, image lag was not felt to be a significant factor influencing the results.

Further details regarding the facility, the apparatus, procedures, and results are given by Brungart (1990).

## DATA REDUCTION PROCEDURES

The attenuation of the intensity, I, of a laser beam passing through a fluorescent dye solution with a concentration, C(moles/liter), where y is the distance (cm) from some reference location, and $\epsilon$ is the extinction coefficient given earlier, is expressed by the Lambert Beer law as:

$$dI(y) = - \epsilon\, C(y)\, I(y)\, dy \tag{1}$$

Parker (1968). The quantum yield of the dye, Q, is the fraction of absorbed photons resulting in fluorescent emission. The local fluorescent signal intensity, $I_f(y)$, is Q times the absorbed fraction of the local excitation beam intensity. Integrating equation (1), an expression for the fluorescent intensity from some small slice, $\Delta y$, of the excitation laser beam is obtained by using the definition of the quantum yield. When $\epsilon\, C(y)\, \Delta y \ll 1$ this is:

$$I_f(y) = Q\, \epsilon\, C(y)\, \Delta y\, I_0 \exp\left(-\epsilon \int_0^y C dy\right) \tag{2}$$

where $I_0$ is the excitation intensity at $y = 0$. In the present experiments, $\epsilon C(y)\Delta y \ll 1$ was always the case. The exponential term in Equation (2) accounts for excitation beam absorption and can be large even though $\epsilon C(y)\Delta y$ may be small everywhere because of the integrated affect over the beam path. The fluorescent radiation is randomly polarized and emitted uniformly in all directions.

The signal strength from this slice of the laser beam imaged onto the i-th pixel element depends on a number of factors such as light collection solid angle, window and lens reflections and imperfections, pixel sensitivity, device gain, magnification, excitation beam intensity, the gate period, and the local dye concentration. The various factors can be lumped together and accounted for through a calibration constant, $A_i$, if the conditions at calibration are the same as during the experiment, Koochefahani (1984). Otherwise, each factor must be identified and separately accounted for. The output signal from the i-th pixel is a number of counts, $N_i$, which is proportional to the fluorescent intensity. Discretizing equation (2) and combining constants, the signal in counts is:

$$N_i = A_i \, C_i \prod_{j=1}^{i-1} \exp(-\epsilon \, C_j \, \Delta y) + B_i \qquad (3)$$

where $B_i$ is the device noise due to spontaneous emission and clock switching noise during the array readout. $B_i$ may also contain the background signal due to dye buildup in the water tunnel. The exponential term in (2) and (3) accounts for absorption of the excitation beam by dye over its path to the slice imaged by the i-th pixel. At sufficiently low dye concentration and short beam path lengths, this attenuation can be neglected. This was the case for all

the diffusion data, where beam attenuation over the field of view of the LIF imaging optics was, at most, approximately 1%. It was only necessary to account for absorption along the beam path when calibrating; the maximum attenuation being approximately 4.5%.

## CALIBRATION

Calibration requires solving (3) for $A_i$ and using measured values of $N_i$ for a known uniform dye concentration C and $B_i$ measured with the background signal. Two calibration procedures have been tried. The first procedure used the water tunnel as a calibration flow cell. The tunnel volume must be known to do this and was determined by dissolving 500g, 1000g, and 2000g of sodium sulfate in the tunnel and comparing the resulting changes in the water conductivity with a reference solution. The three values obtained for the tunnel volume agreed within 0.01%. Knowing the tunnel volume, dye was added to the tunnel to create a uniform dye concentration. However, due to dye absorption of the excitation laser beam, only relatively low concentrations were practical with this calibration procedure. The decay of the fluorescent signals from prepared solutions as they aged, discussed above, could not be calibrated for by this procedure.

The second calibration procedure used a small flow cell placed in the test section at the measurement location. The cell had no bottom surface and sealed against the working surface of the test plate acrylic window when weights were placed on top of it. Thus, the calibration was again performed with the excitation and imaging optics set-up exactly as for the experiments to follow except that reflections off the window on the calibration cell are not accounted for. These reflective losses, however, are less than 1% and were neglected.

Calibrations using the flow cell method were made at dye concentrations ranging from the injection concentration to 1/64 of the injection concentration. These dilution calibrations were made by adding water from the tunnel to samples of the various solutions that were injected into the TBL through the slot. These multiple concentration calibrations were done to verify the expected linear variation of the signal with concentration and to provide some experimental estimate of the error that is likely in the TBL profile measurements. Figure 4 shows the pixel sensitivity in counts per (mole/liter) of dye versus dye concentration at four pixel locations on the array for a typical set of water calibrations. The sensitivity of a given pixel should be constant and the variations about the mean are less than 10%. This is reasonably good considering that the calibration concentrations are estimated as 5% accurate. The major difficulty with this flow cell procedure is bubbles forming on the cell window and bubbles in the flow. With attention to such details, the two calibration procedures produce signals with the same form across the linear array.

## RESULTS

The polymer used was polyethylene oxide with a mean molecular weight, as reported by the manufacturer, of $5 \times 10^6$. Polymer was mixed into tap water that had been allowed to sit for a period of at least two days to reduce possible chlorine degradation effects. Occasional gentle stirring helped hydration of the polymer and the polymer was given at least 18 hours to hydrate.

Polymer injection flowrates are normalized by the flowrate in the viscous sublayer of the pure water boundary layer, $Q_s$, defined by Wu and Tulin (1972) as the flow through the area extending from the wall to $y^+ = 11.6$. This sublayer volumetric flowrate per unit span is 67.3 times the kinematic viscosity of the fluid. This is an interesting result in that the edge of the sublayer, in the mean, is a streamline and the sublayer flowrate is not a function of freestream velocity. $Q_s$ is approximately 4.05 liters/minute/m span in water at room temperature.

Water was injected into the TBL with a freestream velocity of 4.6m/s at flow rates from 2 to $10Q_s$. A diffusion layer thickness, $\lambda$, defined as the height above the wall that the mean concentration decreases to 50% of its maximum value at the measurement streamwise position was determined from the measured mean concentration profiles. Figure 5 shows these $\lambda$ normalized by the local boundary layer thickness, $\delta_{loc}$, versus the streamwise distance from the slot, x, normalized with the average boundary layer thickness between the slot and x, $\delta_{av}$. The solid curve in Figure 5 represents the passive contaminant line source diffusion results of Poreh and Cermak (1964) and the agreement with the present results is excellent. These data span what Poreh and Cermak (1964) term the intermediate and transitional diffusion zones and the most downstream data is slightly upstream of the final diffusion zone. Upstream of the final zone, the diffusion layer grows faster than the viscous boundary layer. In the final zone, both layers grow at the same rate and $\lambda/\delta_{loc} = 0.64$. Figure 6 compares the mean concentration profile of water at $x/\delta_{av} = 2.5$ to an empirical relationship derived by Morkovin (1965). The agreement is excellent which supports that the technique and procedures are working as expected. Similar agreement is

found at the most downstream location using the final zone value of the exponent, a = 2.15, in Morkovin's (1965) curve fit.

Mean concentration profiles at a location 129mm downstream of the slot at $x/\delta_{av}$ = 20.7 are shown in Figure 7 for a 500wppm concentration polyethylene oxide solution injected at various rates with a freestream velocity of 4.6 m/s. Based on the estimated pure water friction velocity at the slot, $u^*$ = 0.195 m/s, this measurement location is at $x^+$ = 25,000, approximately. The microscope magnification was 2.37 and each pixel on the array covers 2.0 viscous wall units vertically based on the pure water scales. The maximum measured concentrations are seen to decrease proportionately with the polymer injection rate except for the $10Q_s$ data. This difference in the $10Q_s$ data is believed to be a saturation affect. Once the local maximum concentration reaches the injection value, it cannot increase further with injection rate. This was observed at the upstream location with the $10Q_s$ injection rate, and this saturation affects the downstream results. For comparison to the water results in Figure 5, Figure 8 shows the 500wppm polyox diffusion layer thickness results. The mass diffusion of the polymer is appreciably slower than that of the water initially. The polymer maintains a concentrated layer on the wall exhibiting what Poreh and Cermak (1964) define as initial zone behavior as far downstream as $x/\delta_{av}$ = 34 for these injection and flow conditions. This is consistent with previous studies (Latto and El Riedy (1976), Fruman and Tulin (1976), Collins and Gorton (1976)). The transition from the initial to the final zone is more abrupt with the polymer. How these characteristics change with concentration, injection rate, and velocity are being studied.

The slight drop in the mean polymer concentration near the wall in Figure 7 is not observed with water injection and is not believed to be real. The size of the measured drop from the maximum value near the wall to the value at the wall increases with polymer concentration and the maxima moves away from the wall as the injection rate is increased. The data taken at the location nearest the slot is most affected. The index of refraction of the polymer solutions are slightly higher than that of water and this may explain this anomaly. At 20°C, the measured indices of refractions for tap water, 500wppm polyethylene oxide and 1000wppm polyethelyene oxide are 1.3306, 1.3308, and 1.3310 respectively. Although these seem like very small differences, ray tracing calculations assuming a discontinuous change in the index of refraction indicate beam deflections due to the index gradient may be as large as 0.3 degrees. This optical aberration defocuses the signal very near the surface. The weak signals reflected off of the surface of the plate are imaged partially by the near wall pixels, and the result is the observed drop off.

The maximum concentration measured at the most upstream location, 12.7mm ($2.5\delta_{SLOT}$) from the slot, at the $10Q_s$ injection rate with a 4.6 m/s freestream velocity was the injection concentration for both water and the 500wppm polymer solution. The water maximum was at the wall. However, the measured polymer maximum was at $y^+ = 23$, approximately, and the concentration dropped 14% to the wall. This extreme case is felt to establish the maximum possible error in the concentration at the wall at this injection concentration due to index of refraction gradients. Assuming that the maximum concentration is representative of the

concentration at the wall should reduce this error and provide a reasonably accurate estimate of the near wall concentration.

Figure 9 shows the standard deviations of the polymer concentration fluctuations under the same conditions as in Figure 7. The standard deviation has a maxima above the wall that diminishes and moves toward the wall with decreasing injection rate and increasing streamswise distance. A part of this decrease near the wall is due to the decreases seen in the mean profiles mentioned above. However, water standard deviation data at the upstream measurement locations have similar maxima indicating that these polymer maxima are real. The observed standard deviation maxima are displaced further from the wall and are larger in relative magnitude than the mean concentration signal decrease due to the index gradient seen in Figure 7. Significant concentration fluctuations occur above $y^+ = 300$ even though the mean profiles in Figure 7 show relatively little polymer this far from the wall.

Figures 10 and 11 show distributions of skewness and flatness factors for the polymer concentration. The skewness factors exhibit a nearly linear increase beginning at the wall from a Gaussian value that continues across the entire field of view which extends to $y^+ = 900$. The skewness factor profiles are more or less the same at all of the injection rates. The flatness factors increase monotonically from Gaussian values near the wall but the increase is not linear. Beyond $y^+ = 350$, which is outside of the diffusion layer, these profiles become irregular due to the highly intermittent character of the extreme edge of the diffusion layer, due to the diminishing size of the standard deviation which is the normalization parameter for these factors and due to statistical uncertainty.

Other analyses may be performed on these concentration data. Probability density functions of the polymer concentration as a function of distance from the wall can be examined under various conditions of injection and flow. The instantaneous profiles show that in the initial diffusion zone the polymer occasionally lifts off the wall in concentrated filaments. This lifting leaves little polymer at the wall locally and should play a fundamental role in the diffusion process in the initial zone. However interesting, the point to take is the utility of the present technique for the study of such problems.

## SUMMARY

A laser induced fluorescence technique for measuring near instantaneous concentration profiles of slot injected fluids in high unit Reynolds number turbulent boundary layers has been presented. Representative results taken with water injection and with drag reducing polymer injection are discussed. Comparison with previous passive contaminant studies support that the current technique works well. The technique makes possible the determination of mean profiles, profiles of higher order central moments, concentration probability density functions as a function of distance from the wall, and details of the line source diffusion process not possible by earlier concentration measurement methods.

## REFERENCES

Bues, M., Reitzer, H. and Scrivener, O., "Diffusion of Macromolecular Solutions in the Turbulent Boundary Layer of a Cylindrical Pipe IV Visualization and Model of Changes Occurring at the Diffusion Boundary Layer," Rheologica Acta, Vol. 24, No. 3, pp 312-316, 1985.

Brungart, T. A., "A Laser-Induced Fluorescence Technique for Measurement of Slot-Injected Fluid Concentration Profiles in a Turbulent Boundary Layer," M.S. Thesis, Department of Mechanical Engineering, The Pennsylvania State University, 1990.

Collins, D. J. and Gorton, C. W., "An Experimental Study of Diffusion From a Line Source in a Turbulent Boundary Layer," AIChE Journal, Vol. 22, No. 3, pp. 610-612, May 1976.

Fruman, D. H. and Tulin, M. P., "Diffusion of a Tangential Drag Reducing Polymer Injection of a Flat Plate at High Reynolds Numbers," Journal of Ship Research, Vol. 20, No. 3, pp. 171-180, September 1976.

Guilbualt, G. G., Practical Fluorescence, Marcel Dekker, Inc., New York, 1973.

Ippen, E. P., Shank, C. V., and Dienes, A., "Rapid Photobleaching of Organic Laser Dyes in Continuously Operated Devices," IEEE Journal of Quantum Electronics, QE-7, pp. 178-179, April 1971.

Koochesfahani, M. M., Experiments on Turbulent Mixing and Chemical Reactions in a Liquid Mixing Layer, Ph.D. thesis, California Institute of Technology, 1984.

Koochesfahani, M. M. and Dimotakis, P. E., "Laser-Induced Fluorescence Measurements of Mixed Fluid Concentration in a Liquid Plane Shear Layer," AIAA Journal, Vol. 23, No. 11, pp. 1700-1707, November 1985.

Latto, B. and El Riedy, O., "Diffusion of Polymer Additives in a Developing Turbulent Boundary Layer," Journal of Hydronautics, Vol. 10, No. 4, pp. 135-139, October 1976.

Lumley, J. L., "Drag Reduction in Turbulent Flow by Polymer Additives," Journal of Polymer Science, Macromolecular Reviews, Vol. 7, pp. 283-290, 1973.

Lumley, J. L., "Drag Reduction in Two Phase and Polymer Flows," Phys. of Fluids, Supplement, Vol 20, No. 10, October 1977, pp. S64-S71.

Morkovin, M. V., "On Eddy Diffusivity, Quasisimilarity and Chemical Reactions in Turbulent Boundary Layers," Int. J. Heat Mass Transfer, Vol 8, pp. 129-145.

Parker, C. A., Photoluminescences of Solutions, Elsevier, New York, 1968.

Poreh, M. and Cermak, J. E., "Study of Diffusion from a Line Source in a Turbulent Boundary Layer," Int. Journal of Heat Mass Transfer, Vol. 7, pp. 1083-1095, 1964.

Tiederman, W. G., Walker, D. T., and Bustetter, D. C., "Injection of Drag Reducing Additives into Turbulent Water Flows, Mixing Experiments and Newtonian Burst Frequency," Report PME-FM-87-1, Purdue University, 1987.

Toms, B. A., "Some Observations on the Flow of Linear Polymer Solutions through Straight Tube at Large Reynolds Numbers," In Proceedings 1st Int. Rheol Congress, North Holland Publishing Co., Vol. 11, pt. 2, pp. 135-142, 1949.

Vdovin, A. V. and Smol'yakov, A. V., "Diffusion of Polymer Solutions in a Turbulent Boundary Layer," Translated from Zhurnal Prikladnoi Mekhaniki i Tekhnicheskoi Fiziki, No. 2, pp. 66-73, March-April, 1978.

Vdovin, A. V. and Smol'yakov, "Turbulent Diffusion of Polymers in a Boundary Layer," Translated from Zhurnal Prikladnoi Mekhaniki i Tekhnicheskoi Fiziki, No. 4, pp. 98-104, July-August, 1981.

Walker, D. A., "A Fluorescence Technique of Measurements of Concentration in Mixing Liquids," Journal of Physics E: Science Instru., Vol. 20, pp. 217-224, 1987.

Walker, D. T. and Tiederman, W. G., "A Concentration Field in a Turbulent Channel Flow With Polymer Injection at the Wall," Experiments in Fluids, Vol. 8, pp. 86-94, 1990.

Walker D. T. and Tiederman, W. G., "Injection of Drag Reducing Additives into Turbulent Water Flows - Concentration Results from Time Resolved Measurements," Report PME-FM-88-1, Purdue University, 1988.

Wetzel, J. M. and Ripken, J. F., "Shear and Diffusion in a Large Boundary Layer Injected with Polymer Solution," Project Report No. 114, St. Anthony Falls Hydraulic Laboratory, University of Minnesota, 1970.

Wick, R. A., "Quantum Limited Imaging Using Microchannel Plate Technology," Applied Optics, Vol. 26, No. 16, pp. 3210-3218, August 1987.

Wu, J. and Tulin, M. P., "Drag Reduction by Ejecting Additive Solutions into Pure Water Boundary Layer," Transaction of the ASME, Journal of Basic Engineering, Vol 94D, pp. 749-756, December 1972.

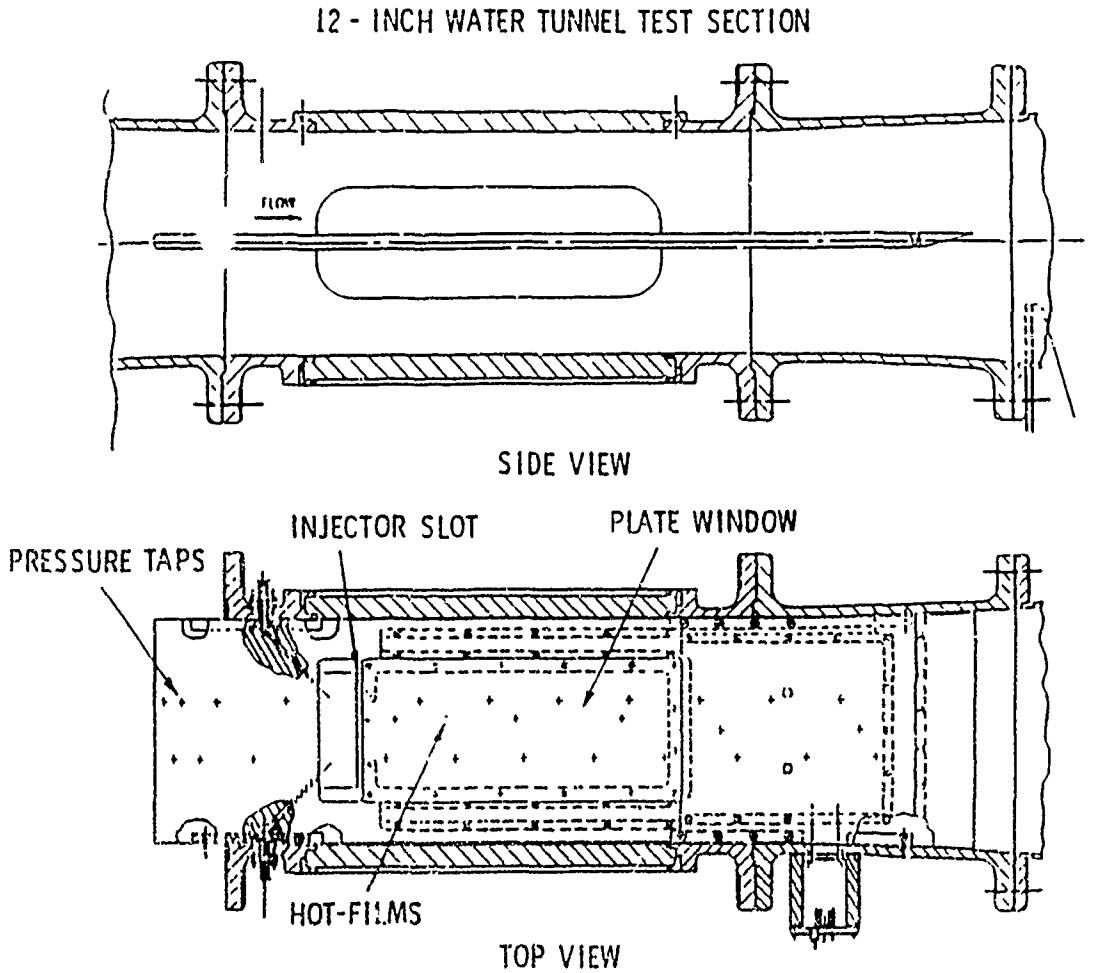


Figure 1. Scale Diagram of Flat Plate Mounted in 0.305m Diameter Water Tunnel Test Section

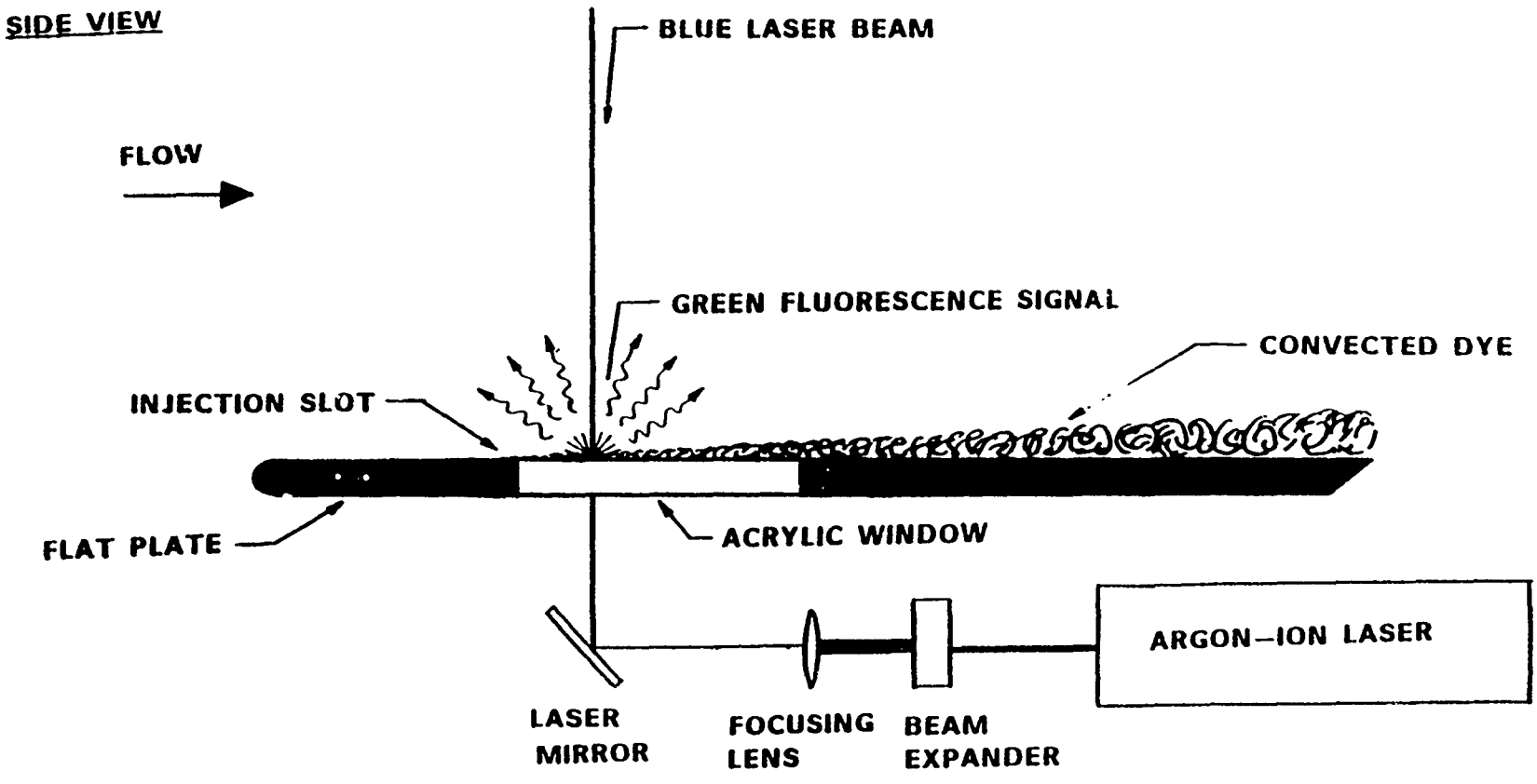


Figure 2. LIF Excitation Optics

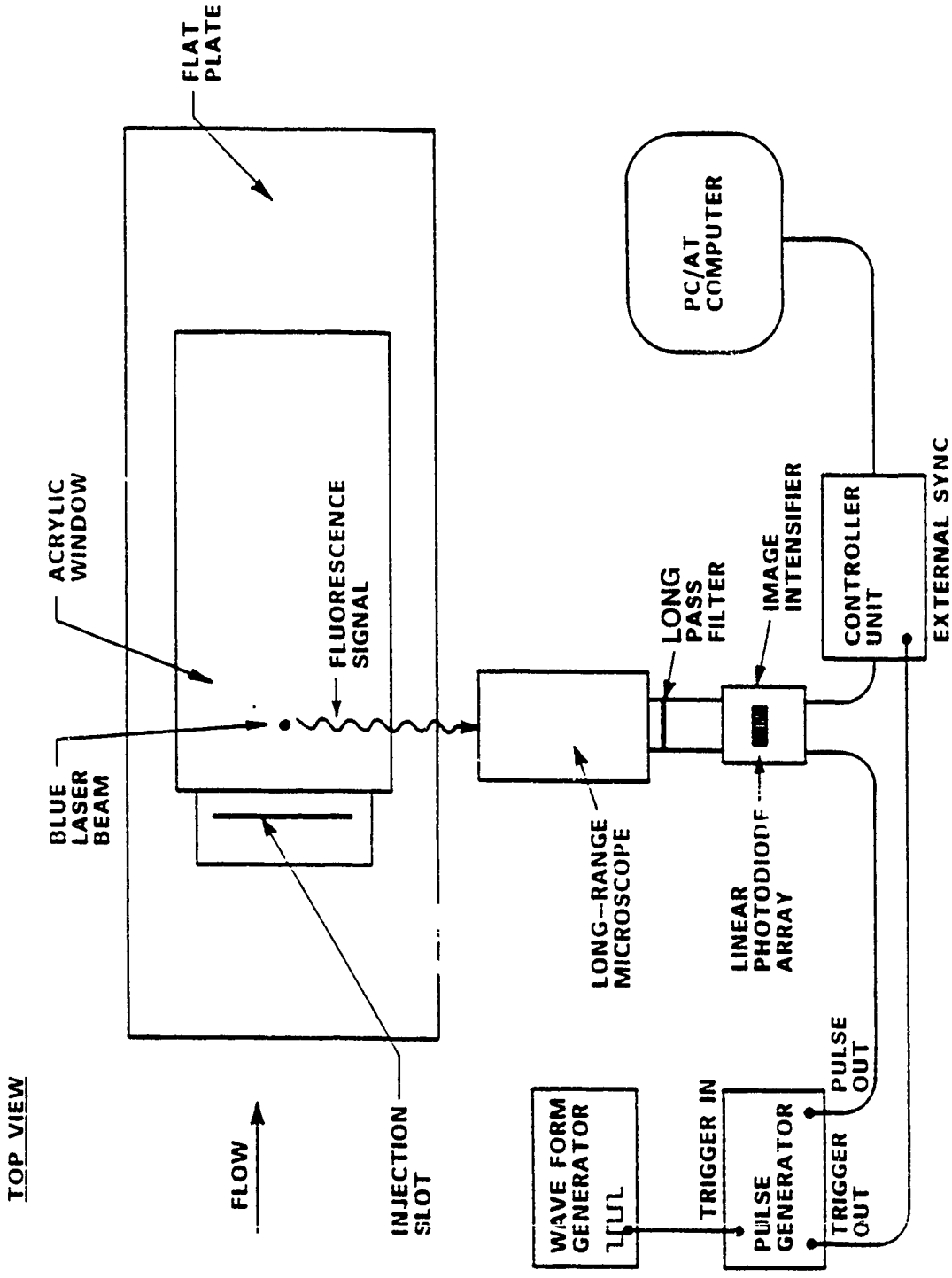


Figure 3. LIF Imaging Optics, Electro-Optics, and Electronics

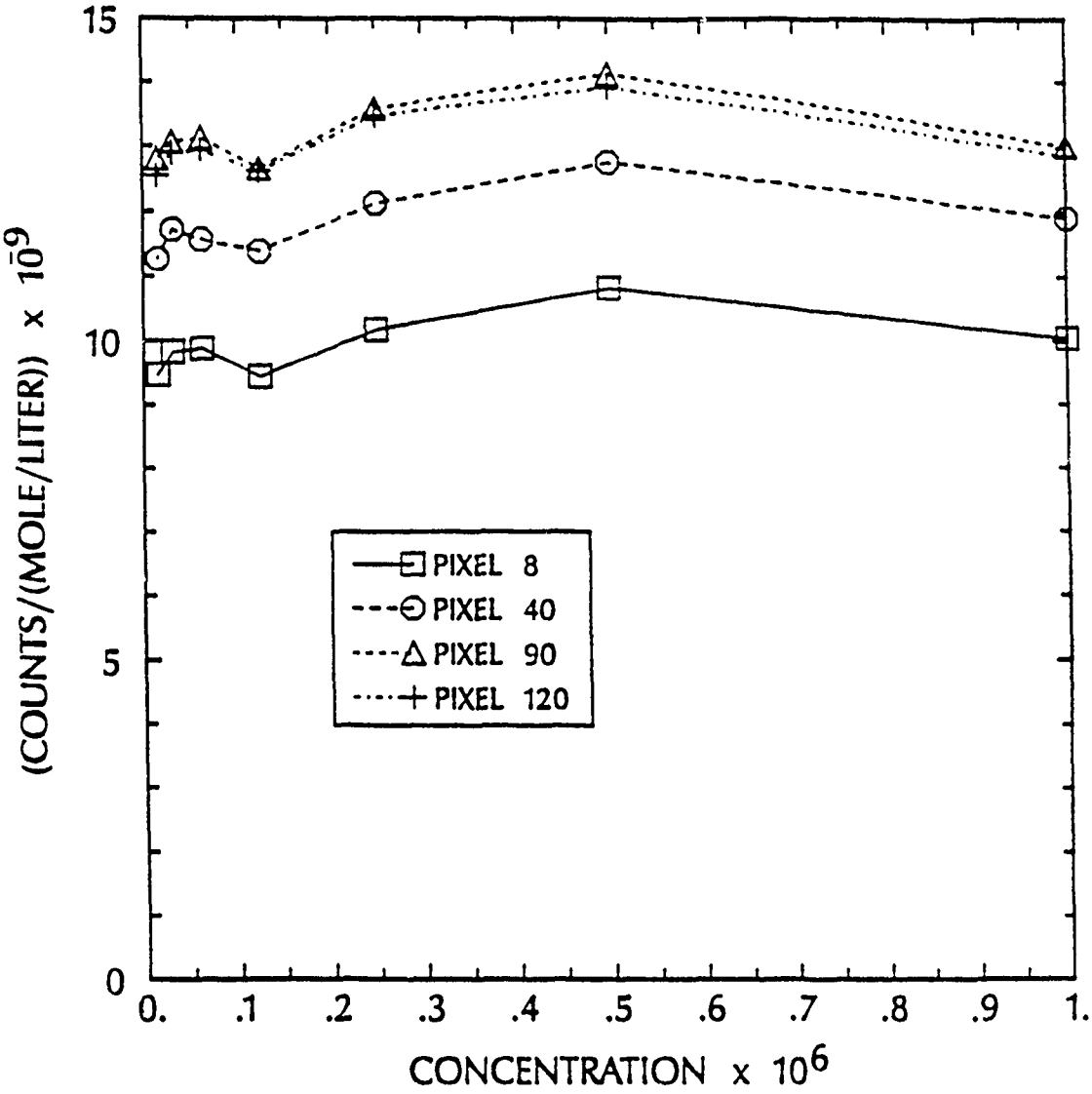


Figure 4. Pixel Sensitivities Determined From Flow Cell Calibrations for a Range of Dye Concentrations

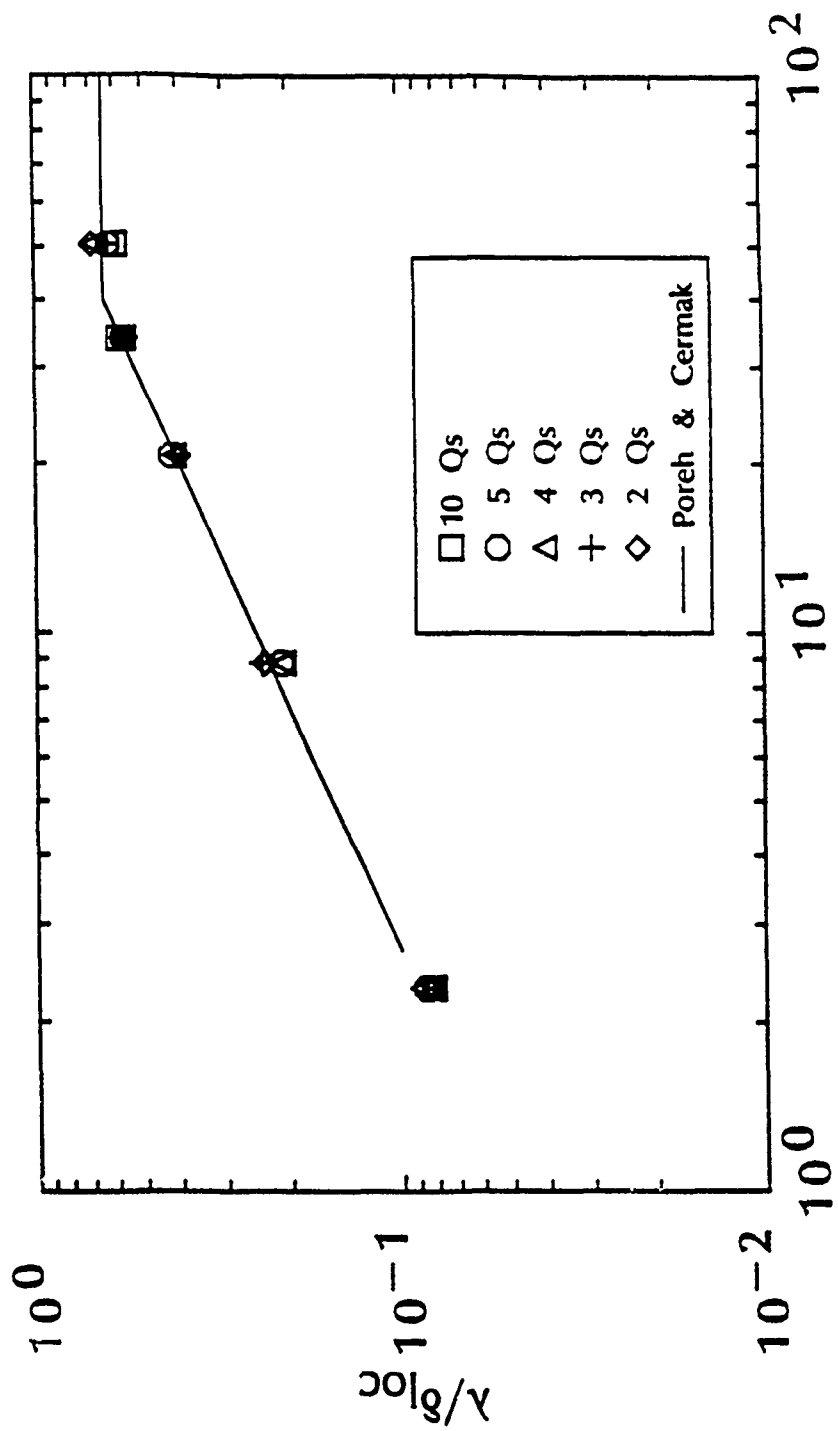


Figure 5. Diffusion to Viscous Boundary Layer Thickness Ratio Versus Streamwise Position With Water Injection, U = 4.6m/s

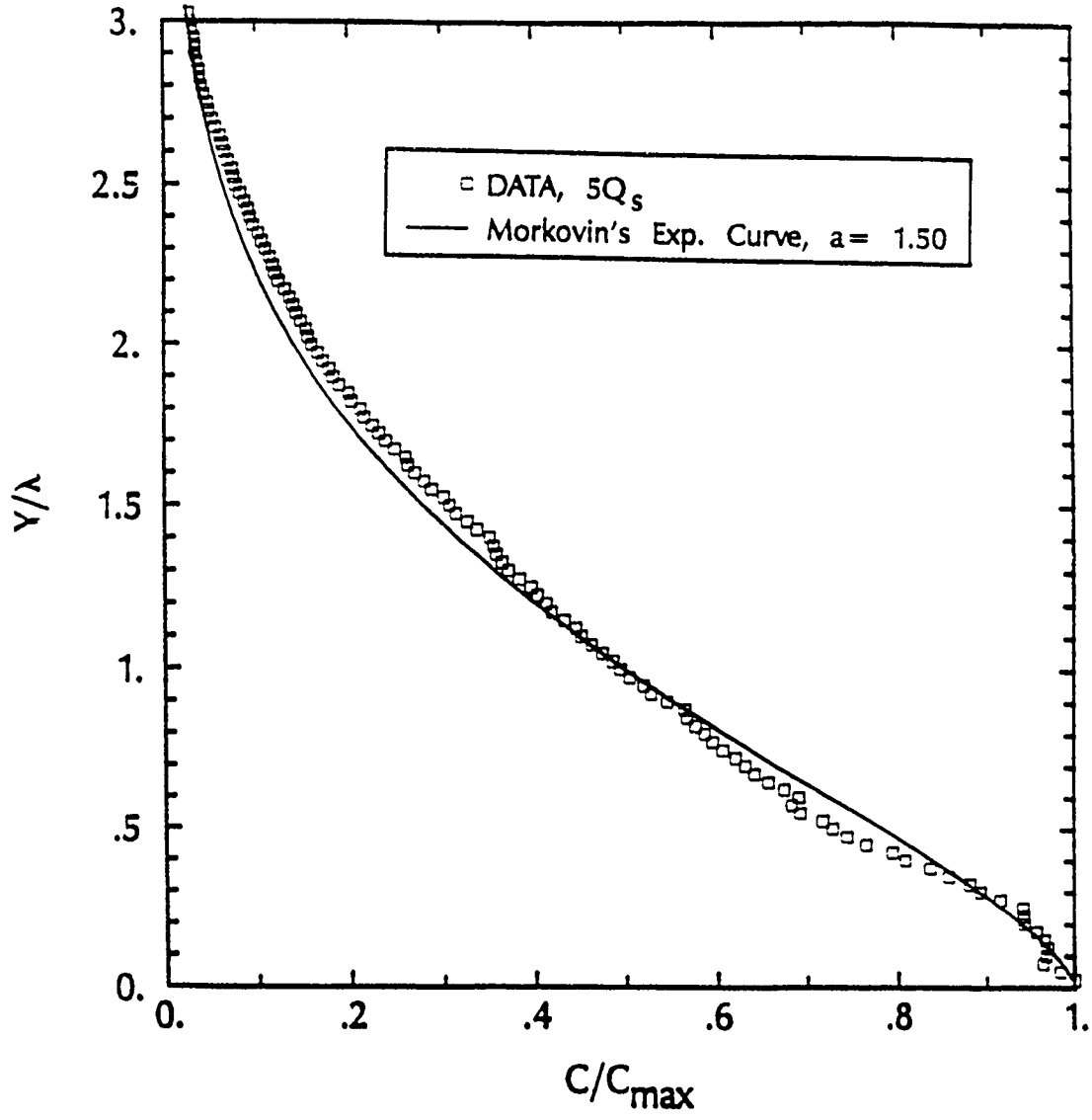


Figure 6. Comparison of Mean Concentration Profiles With Water Injection at $x/\delta_{av}$ = 2.3 With the Intermediate Diffusion Zone Mean Profile of Morkovin (1965)

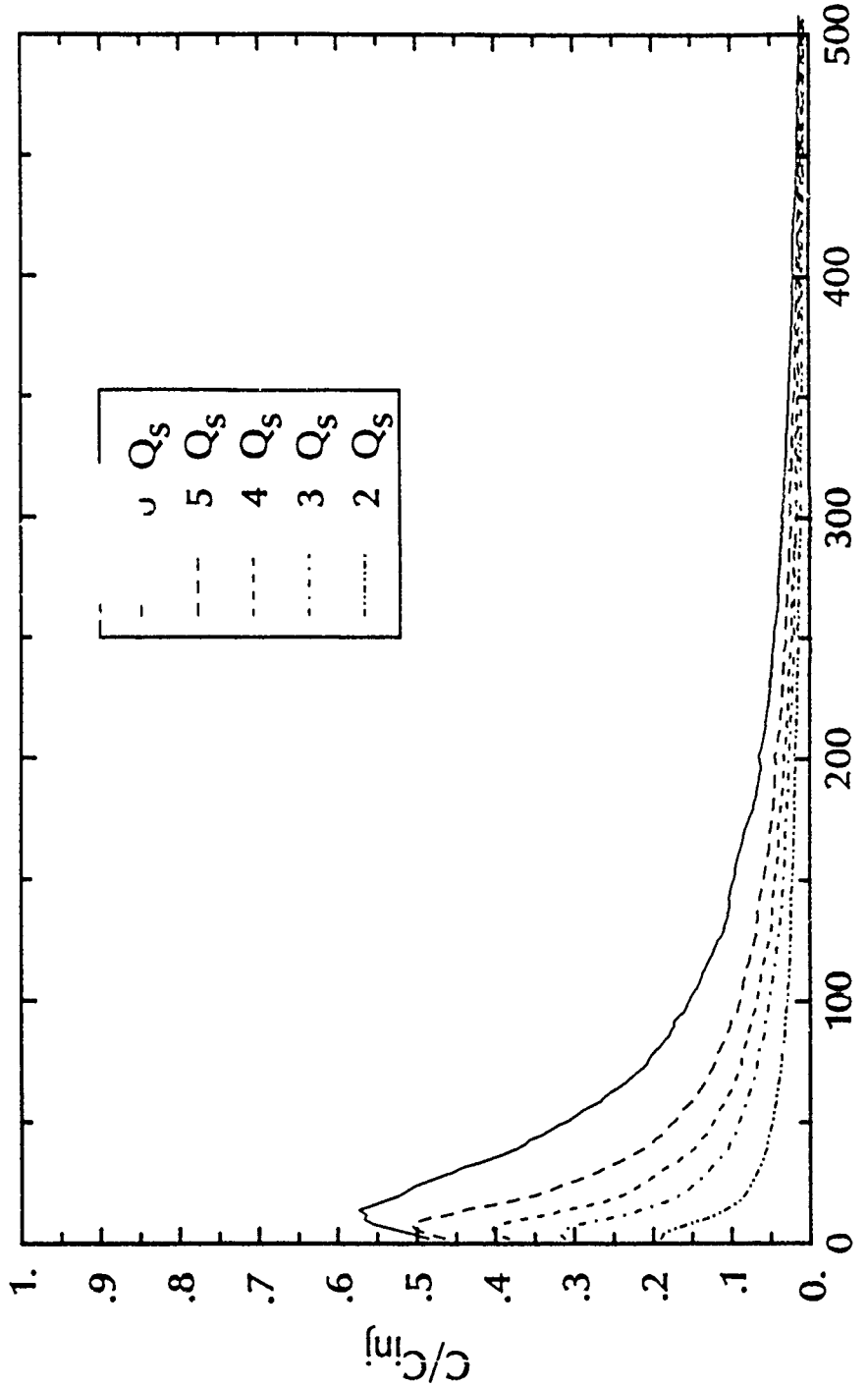


Figure 7. Polymer Mean Concentration Profiles at U = 4.6m/s, $C_{inj}$ = 500wppm, x = 129mm, $x/\delta_{av}$ = 20.7

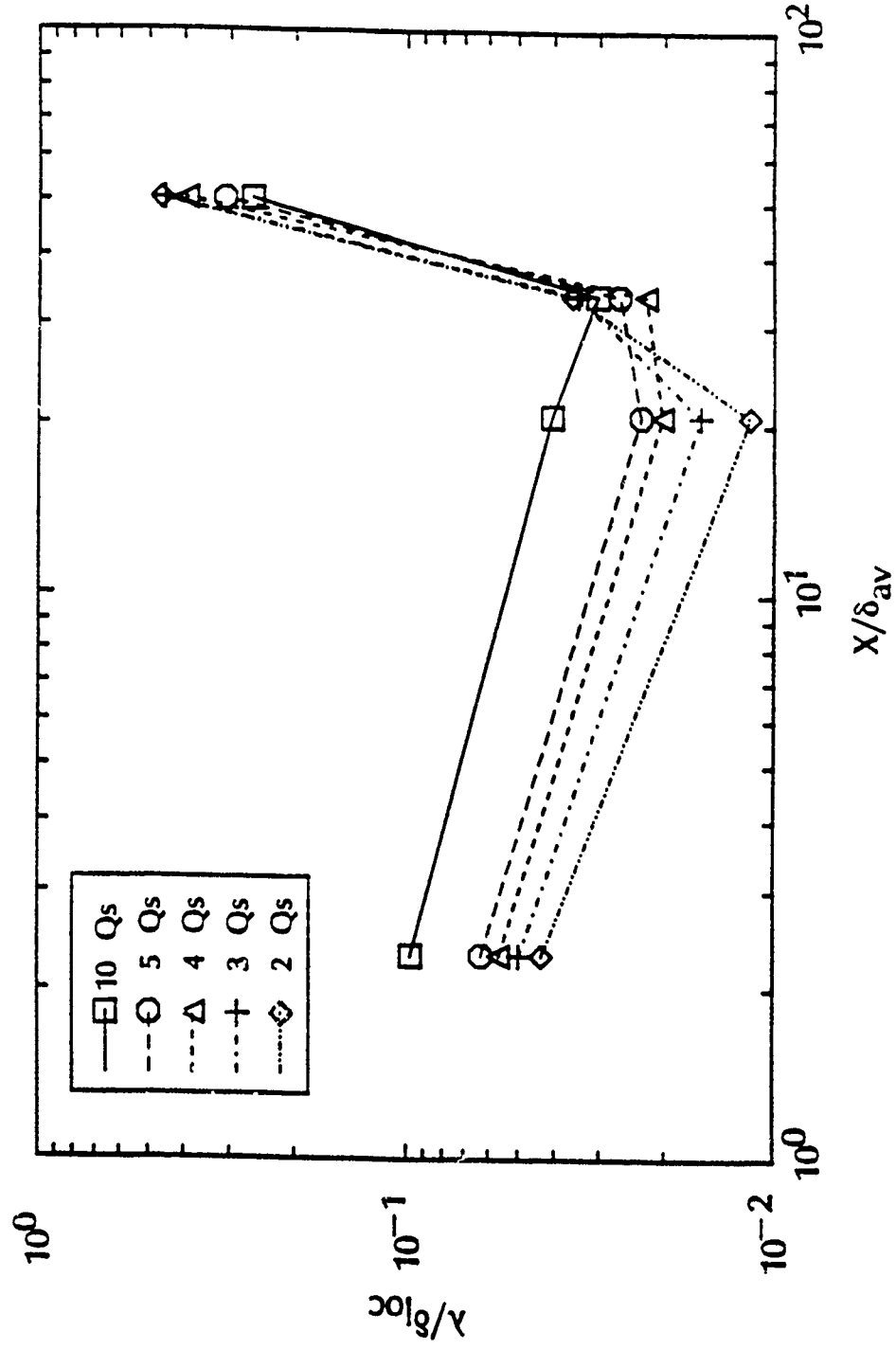


Figure 8. Polymer Diffusion to Viscous Boundary Layer Thickness Ratios Versus Streamwise Position, $C_{inj}$ = 500wppm, U = 4.6m/s

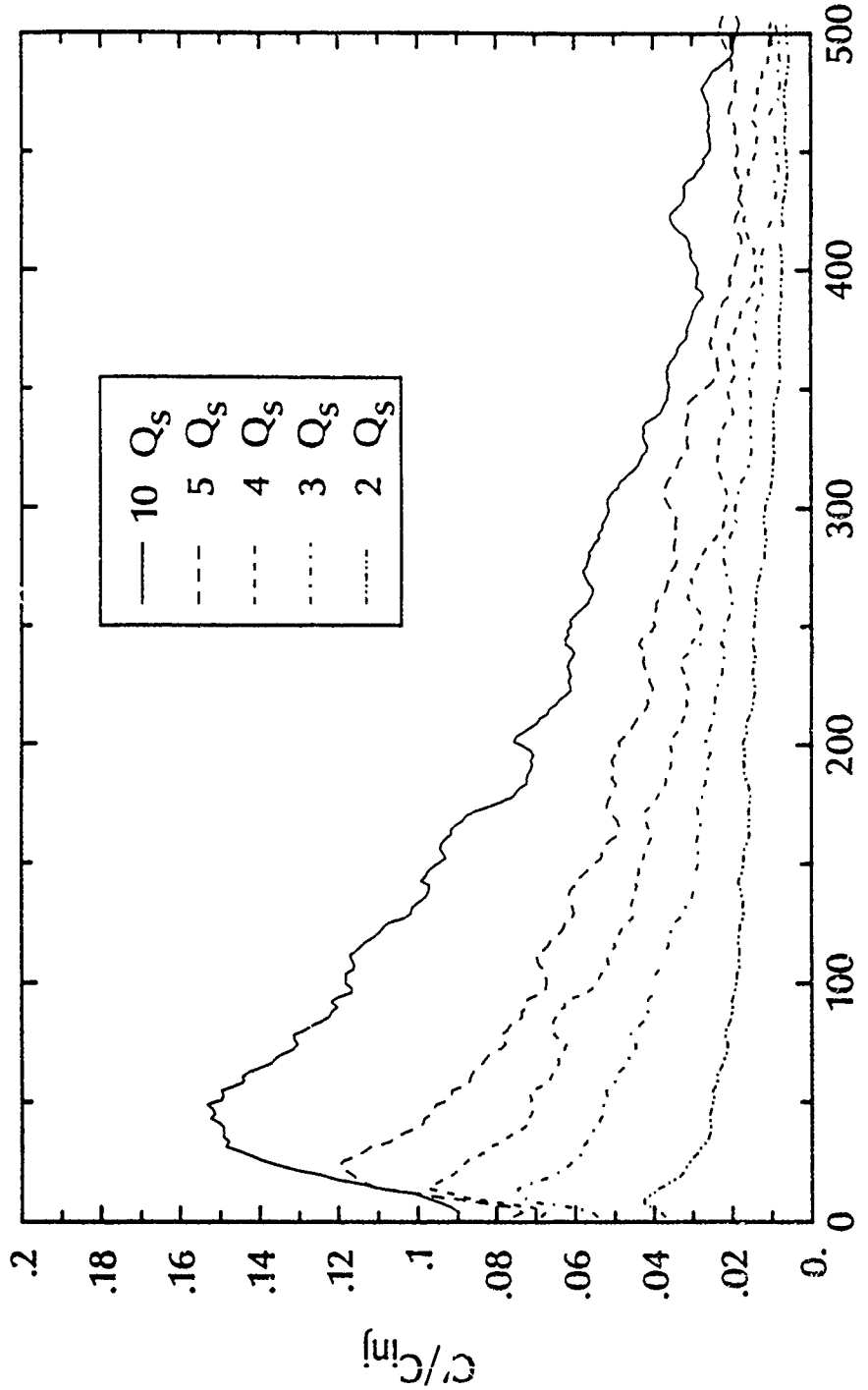


Figure 9. Polymer Concentration Standard Deviation Profiles at $\bar{U}$ = 4.6m/s, $C_{inj}$ = 500wppm, $x/\delta_{av}$ = 20.7

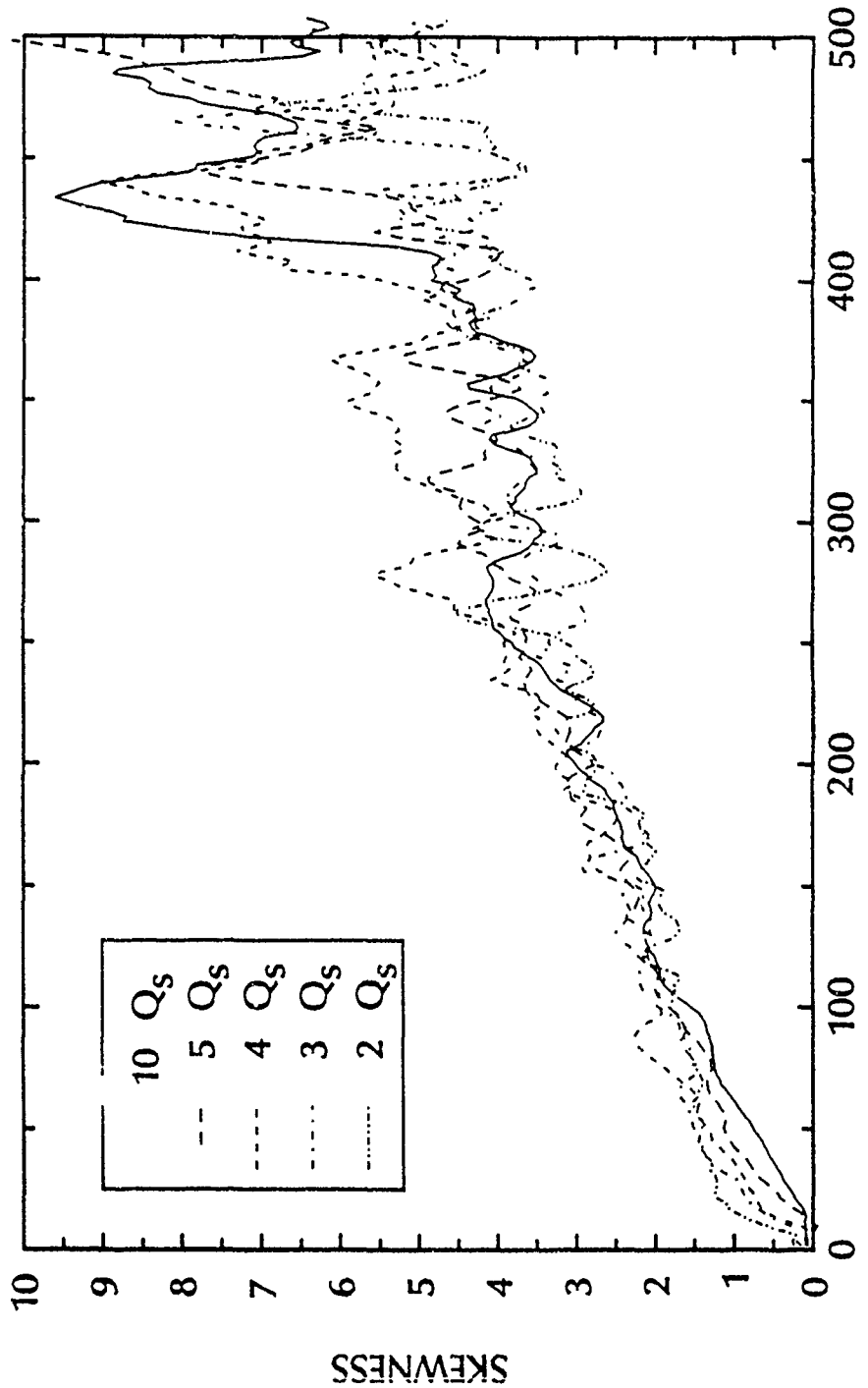


Figure 10. Polymer Concentration Skewness Factor Profiles at U = 4.6m/s, $C_{inj}$ = 500wppm, $x/\delta_{av}$ = 20.7

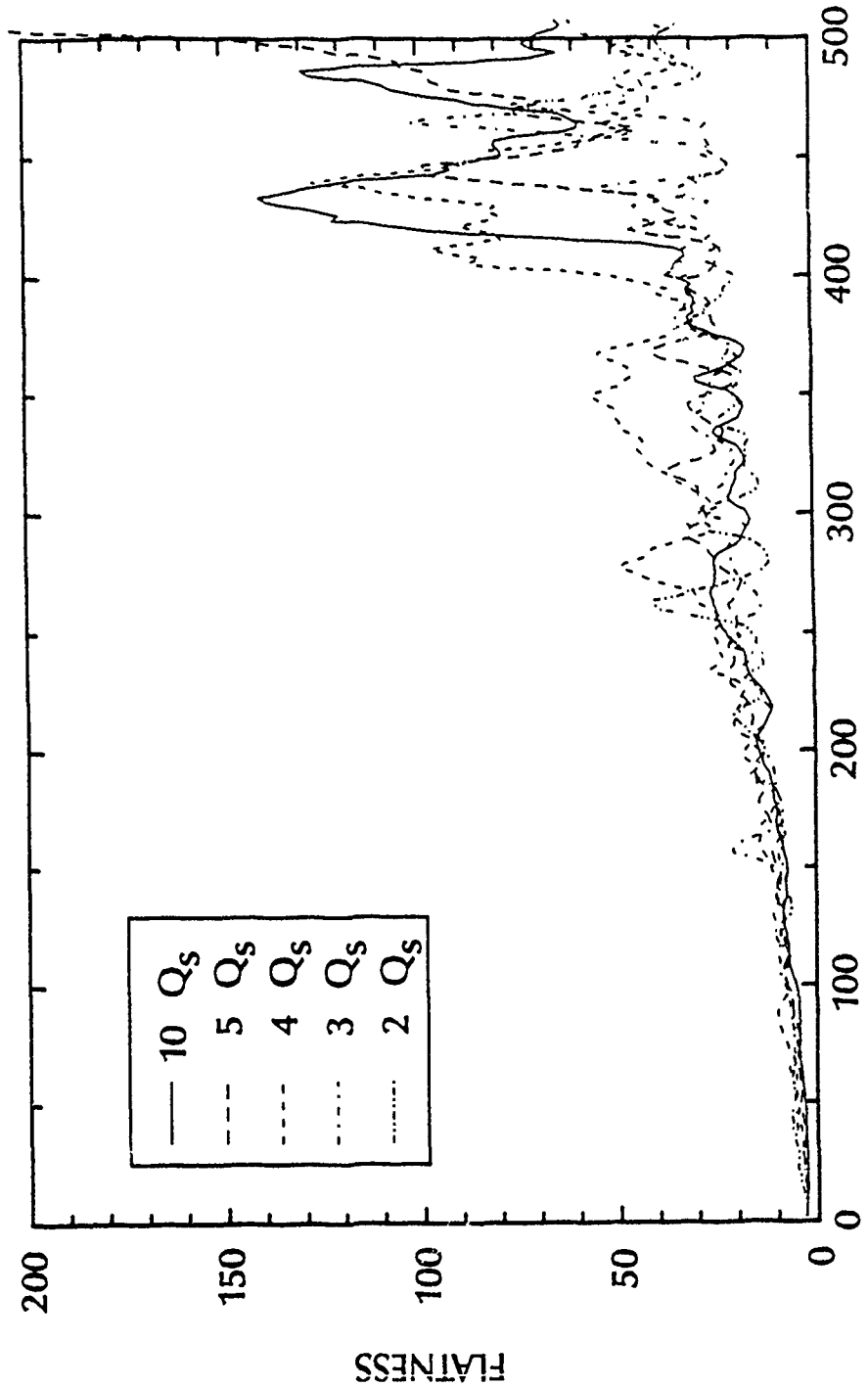


Figure 11. Polymer Concentration Flatness Factor Profiles at $U = 4.6m/s$, $C_{inj} = 500wppm$, $x/\delta_{av} = 20.7$

DISTRIBUTION LIST FOR ARL UNCLASSIFIED TM 90-197 by T. A. Brungart and H. L. Petrie dated 27 August 1990.

Commander Officer
Office of Naval Research
800 N. Quincy Street
Arlington, VA 22217
Attn: J. A. Fein
Code 1215
(Copy No. 1)

Commanding Officer
Office of Naval Research
Attn: R. J. Hansen
Code 1243
(Copy No. 2)

Commanding Officer
Office of Naval Research
Attn: A. D. Wood
Code ONR 12
(Copy No. 3)

Commanding Officer
Office of Naval Research
Attn: E. P. Rood
Code 1132F
(Copy No. 4)

Commanding Officer
Office of Naval Research
Attn: M. M. Reischman
Code 1132F
(Copy No. 5)

Defense Technical Information
Center (12)
Cameron Station
Alexandria, VA 22304-6145
Attn: DTIC-DDA
(Copy No. 6)

Commanding Officer
Office of Naval Technology
800 North Quincy Street
Arlington, VA 22217-5000
Attn: A. J. Faulstich
Code OCNR-23
(Copy No. 7)

Commanding Officer
Office of Naval Technology
Attn: D. C. Houser
Code ONT232
(Copy No. 8)

Commanding Officer
Naval Underwater Systems Center
Department of the Navy
Newport, RI 02841-5047
Attn: R. D. Nadolink
Code 3634
(Copy No. 9)

Commanding Officer
Naval Underwater Systems Center
Attn: R. B. Philips
Code 8214
(Copy No. 10)

Commanding Officer
Naval Underwater Systems Center
Attn: D. Goodrich
Code 3634
(Copy No. 11)

Commanding Officer
Naval Underwater Systems Center
Attn: D. Brown
Code 3634
(Copy No. 12)

Department of Ocean Engineering
Massachusetts Institute of Tech.
77 Massachusetts Ave.
Cambridge, MA 02139
Attn: P. Leehy
(Copy No. 13)

Sibley School of Mech. & Aero.
Engineering
Upson Hall
Cornell University
Ithaca, NY 14850
Attn: J. L. Lumley
(Copy No. 14)

Commanding Officer
David Taylor Research Center
Department of the Navy
Bethesda, MD 20084
Attn: J. H. McCarthy
Code 154
(Copy No. 15)

Commanding Officer
David Taylor Research Center
Attn: V. J. Monacella
Code 1504
(Copy No. 16)

David Taylor Research Center
Attn: W. Souders
Code 1543
(Copy No. 17,18,19)

Department of Aerospace Engr.
Virginia Polytechnic Institute
and State University
Blacksburg, VA 24061
Attn: Prof. R. L. Simpson
(Copy No. 20)

Department of Mechanical Engr.
Thermosciences Division
Stanford University
Stanford, CA 94305
Attn: Prof. J. P. Johnston
(Copy No. 21)

Department of Mechanical and
Ocean Engineering
University of Rhode Island
Kingston, RI 02881
Attn: Prof. F. M. White
(Copy No. 22)

Division of Engr. & Appl. Sci.
California Institute of
Technology
Pasadena, CA 91125
Attn: A. J. Acosta
(Copy No. 23)

Department of Mechanical Engr.
and Mechanics
354 Packard Laboratory, 19
Lehigh University
Bethlehem, PA 18015
Attn: Prof. D. A. Walker
(Copy No. 24)

Department of Mechanical Engr.
Purdue University
West Lafayette, IN 47907
Attn: Prof. W. Tiederman
(Copy No. 25)

Department of Aerospace and
Mechanical Engineering
Notre Dame University
Notre Dame, IN 46556-9956
Attn: Prof. Mohammad Gadelhak
(Copy No. 26)

Department of Aerospace Engr.
University of Southern California
at Los Angeles
University Park
Los Angeles, CA 90089-0192
Attn: Prof. Ron Blackwelder
(Copy No. 27)

Commanding Officer
Defense Advanced Research
Projects Agency (DARPA)
AB, Architect Building
1400 Wilson Boulevard
Arlington, VA 22209-2308
Attn: Gary Jones
(Copy No. 28)

Commanding Officer
Naval Ocean Systems Center
Department of the Navy
San Diego, CA 92152
Attn: T. Mautner
Code 6432
(Copy No. 29)

NASA Lewis Research Center
21000 Brookpark Rd.
Cleveland, OH 44135
Attn: N. Sanger
Code MS 60-5
(Copy No. 30)

NASA Langley Research Center
MS163
Hampton, VA 23665
Attn: Ben Anders
(Copy No. 31,32)

Applied Researach Laboratory
Penn State University
P.O. Box 30
State College, PA 16804
Attn: H. L. Petrie
(Copy No. 33)

Applied Research Laboratory
Attn: ARL Library
(Copy No. 34)

Applied Research Laboratory
Attn: GTWT Files
(Copy No. 35)